AEM
Journals.ASM.org

Quantitative Microbial Ecology through Stable Isotope Probing

Bruce A. Hungate,[a,b] Rebecca L. Mau,[a] Egbert Schwartz,[a,b] J. Gregory Caporaso,[a,b,c] Paul Dijkstra,[a,b] Natasja van Gestel,[a] Benjamin J. Koch,[a] Cindy M. Liu,[d,e] Theresa A. McHugh,[a*] Jane C. Marks,[a,b] Ember M. Morrissey,[a] Lance B. Price[d,f]

Center for Ecosystem Science and Society, Northern Arizona University, Flagstaff, Arizona, USA[a]; Department of Biological Sciences, Northern Arizona University, Flagstaff, Arizona, USA[b]; Center for Microbial Genetics and Genomics, Northern Arizona University, Flagstaff, Arizona, USA[c]; Translational Genomics Research Center, Flagstaff, Arizona, USA[d]; Department of Pathology, Johns Hopkins School of Medicine, Baltimore, Maryland, USA[e]; Department of Environmental and Occupational Health, Milken Institute School of Public Health, George Washington University, Washington, DC, USA[f]

Bacteria grow and transform elements at different rates, and as yet, quantifying this variation in the environment is difficult. Determining isotope enrichment with fine taxonomic resolution after exposure to isotope tracers could help, but there are few suitable techniques. We propose a modification to stable isotope probing (SIP) that enables the isotopic composition of DNA from individual bacterial taxa after exposure to isotope tracers to be determined. In our modification, after isopycnic centrifugation, DNA is collected in multiple density fractions, and each fraction is sequenced separately. Taxon-specific density curves are produced for labeled and nonlabeled treatments, from which the shift in density for each individual taxon in response to isotope labeling is calculated. Expressing each taxon's density shift relative to that taxon's density measured without isotope enrichment accounts for the influence of nucleic acid composition on density and isolates the influence of isotope tracer assimilation. The shift in density translates quantitatively to isotopic enrichment. Because this revision to SIP allows quantitative measurements of isotope enrichment, we propose to call it quantitative stable isotope probing (qSIP). We demonstrated qSIP using soil incubations, in which soil bacteria exhibited strong taxonomic variations in ^{18}O and ^{13}C composition after exposure to [^{18}O]water or [^{13}C]glucose. The addition of glucose increased the assimilation of ^{18}O into DNA from [^{18}O]water. However, the increase in ^{18}O assimilation was greater than expected based on utilization of glucose-derived carbon alone, because the addition of glucose indirectly stimulated bacteria to utilize other substrates for growth. This example illustrates the benefit of a quantitative approach to stable isotope probing.

The types of organisms present in an ecosystem profoundly influence its functioning, an idea well established for plants and animals, formalized in the state factor theory of ecosystem science (1), and illustrated through the impacts of plant and animal invasions on ecosystem processes (2). The physiological and taxonomic diversity of microorganisms far exceeds that of plants and animals combined (3). Yet, despite progress in applying molecular tools to analyze the microbial diversity of intact assemblages (4–6), our understanding of how individual microbial taxa affect ecosystem processes like element cycling remains weak. When applied to intact microbial assemblages, stable isotope probing (SIP) partly addresses this challenge, in that it physically links the fluxes of elements to an organism's genome. In conventional SIP, organisms that utilize isotopically labeled substrates incorporate the heavy isotope into their nucleic acids, increasing the density of those nucleic acids, which then migrate further along a cesium chloride density gradient formed during isopycnic centrifugation. This enables the organisms that utilized the labeled compound for growth to be identified (7). Conventional SIP applications use a qualitative approach that uses visual identification of the separation caused by isotope incorporation (7). The nucleic acids in density regions defined as "heavy" or "light" are then sequenced. Organisms disproportionately represented in the heavy region are interpreted as having utilized the labeled substrate for growth (8–11).

SIP is a robust technique to identify microbial populations that assimilate a labeled substrate, but it does not provide quantitative measures of assimilation rates, for three reasons. First, the distinction between labeled and unlabeled organisms is binary, defined by the density regions selected by the investigator, limiting the resolution of taxon-specific responses to labeled or unlabeled. Second, the distribution of DNA along the density gradient reflects the influences of both isotope incorporation and GC (guanine-plus-cytosine) content, because the density of DNA increases with its GC content (12). Any comparison of density regions will reflect both influences, challenging inferences about quantitative isotope incorporation. Third, in conventional SIP, there are no assurances that the identification of the labeled community is complete. Low-GC-content organisms that incorporated the isotope label may not have shifted sufficiently in density to be part of the labeled density fraction, and high-GC-content organisms that did not incorporate the label may be erroneously inferred to be part of the labeled community. This could result in incomplete coverage when discrete, noncontiguous density intervals representing heavy and light fractions (13, 14) are selected for sequencing, omitting information about the microbial assemblage contained in the DNA at intermediate densities. In other cases, only the heavy fractions in both labeled and unlabeled treat-

Received 16 July 2015 **Accepted** 17 August 2015

Accepted manuscript posted online 21 August 2015

Citation Hungate BA, Mau RL, Schwartz E, Caporaso JG, Dijkstra P, van Gestel N, Koch BJ, Liu CM, McHugh TA, Marks JC, Morrissey EM, Price LB. 2015. Quantitative microbial ecology through stable isotope probing. Appl Environ Microbiol 81:7570–7581. doi:10.1128/AEM.02280-15.

Editor: P. D. Schloss

Address correspondence to Bruce A. Hungate, Bruce.Hungate@nau.edu.

* Present address: Theresa A. McHugh, U.S. Geological Survey, Southwest Biological Science Center, Moab, Utah, USA.

Supplemental material for this article may be found at http://dx.doi.org/10.1128/AEM.02280-15.

ments were sequenced and compared: any new organisms that appeared in the heavy fraction of the labeled treatment were inferred to have taken up enough of the isotope tracer to have shifted the density of their DNA (15). This approach could have excluded organisms that incorporated the isotope tracer but, because of their low GC content, did not shift sufficiently to be represented in the heavy fraction. In these ways, SIP as typically practiced is a qualitative technique capable of identifying some of the organisms that utilize a substrate and not a quantitative one capable of exploring the full range of variation in isotope incorporation among microbial taxa.

Here, we describe modifications to SIP that enable isotopic incorporation into the genomes of individual taxa to be quantified. We developed an approach that quantifies the baseline densities of the DNA of individual taxa without exposure to isotope tracers and then quantifies the change in DNA density of each taxon caused by isotope incorporation. Using a model of isotope substitution in DNA, we convert the observed change in density to isotope composition. We show how qSIP applies in soil incubations using a specific carbon source ([^{13}C]glucose) and using a universal substrate for growing organisms ([^{18}O]water). We also show how combining these tracers provides insight into the microbial ecology of a biogeochemical phenomenon widely observed in soil, called the "priming effect" (16). The priming effect is the phenomenon where "extra decomposition of native soil organic matter in a soil receiving an organic amendment" occurs (17) and was first documented over 80 years ago (18–20). The opposite can also be found, where the addition of substrate suppresses organic matter mineralization (21). Some hypotheses to explain priming invoke microbial biodiversity (22), and yet, those controls remain cryptic, in part because of the difficulty of identifying organisms that respond indirectly to the addition of substrate by increasing the decomposition of native soil organic matter. Quantitative SIP has the potential to address these phenomena, by parsing out the contributions of specific microorganisms to the decomposition of the added substrate, labeled with ^{13}C, and to the decomposition of native soil organic matter, which an [^{18}O]water label can detect. Furthermore, the determination of taxon-specific isotope enrichment for each element in qSIP lays the foundation for ascribing rates of element fluxes to particular organisms, which could help explain C fluxes in priming, typically measured on a soil mass basis (e.g., μg C g^{-1} soil^{-1} day^{-1}). In this way, this example illustrates the potential of qSIP to advance microbial ecology as a quantitative field, relating microbial biodiversity to element cycling at the ecosystem scale.

(This article was submitted to an online preprint archive [23].)

MATERIALS AND METHODS

Soil incubations and DNA extractions. Our sample processing scheme, from soil collection, nucleic acid extraction, and centrifugation to data analysis, is summarized in Fig. 1. Soil (0 to 15 cm) was collected in November 2012 from a ponderosa pine forest meadow, located on the C. Hart Merriam Elevation Gradient in northern Arizona (35.42°N, 111.67°W; http://nau.edu/ecoss/what-we-do/future-ecosystems/elevation-gradient-experiment/). Soil was sieved (2-mm mesh), left to air dry for 96 h, and then stored at 4°C before the experiment started. Amounts of 1 g of soil were added to 15-ml Falcon tubes and adjusted to 60% water holding capacity, incubated for 1 week, and then allowed to air dry for 48 h prior to the addition of isotopes. Samples were incubated for 7 days.

During the incubation, samples received 200 μl of water per gram of soil or a glucose solution at a concentration of 500 μg C g^{-1} soil in the following isotope and substrate treatments ($n = 3$ for each): treatment 1, water at natural abundance δ^{18}O; treatment 2, ^{18}O-enriched water (atom fraction 97%); treatment 3, glucose and water at natural abundance δ^{13}C and δ^{18}O; treatment 4, ^{13}C-enriched glucose (atom fraction 99%) and water at natural abundance δ^{18}O; and treatment 5, glucose at natural abundance δ^{13}C and ^{18}O-enriched water (atom fraction 97%). These treatments were selected in order to evaluate the effects of isotope addition on the density and isotopic composition of DNA. We assessed (i) the effect of ^{18}O in the absence of supplemental glucose as the difference between treatments 2 and 1, (ii) the effect of ^{13}C in the presence of supplemental glucose as the difference between treatments 4 and 3, and (iii) the effect of ^{18}O with supplemental glucose as the difference between treatments 5 and 3. In each case, these comparisons isolate the effect of the presence of an isotope tracer. The specific equations quantifying these comparisons are presented below.

After the incubation, samples were frozen and stored at −40°C. DNA was extracted from approximately 0.5 g soil using a FastDNA spin kit for soil (MP Biomedicals, Santa Ana, CA, USA) following the manufacturer's directions. Extracted DNA was quantified using the Qubit double-stranded DNA (dsDNA) high-sensitivity assay kit and a Qubit 2.0 fluorometer (Invitrogen, Eugene, OR, USA).

Density centrifugation and fraction collection. To separate DNA by density, 5 μg of DNA was added to approximately 2.6 ml of a saturated CsCl and gradient buffer (200 mM Tris, 200 mM KCl, 2 mM EDTA) solution in a 3.3-ml OptiSeal ultracentrifuge tube (Beckman Coulter, Fullerton, CA, USA). The final density of the solution was 1.73 g cm^{-3}. The samples were spun in an Optima Max benchtop ultracentrifuge (Beckman Coulter, Fullerton, CA, USA) using a Beckman TLN-100 rotor at 127,000 × *g* for 72 h at 18°C. After centrifugation, the density gradient was divided into fractions of 150 μl each using a fraction recovery system (Beckman Coulter, Inc., Palo Alto, CA, USA). The density of each fraction was subsequently measured with a Reichert AR200 digital refractometer (Reichert Analytical Instruments, Depew, NY, USA). We did not include DNA standards of known GC content in each ultracentrifuge tube. Such standards are traditionally included when computation of GC content based on density is the primary goal (e.g., see references 12 and 24) but are not typically included in SIP studies (25).

DNA was separated from the CsCl solution using isopropanol precipitation, resuspended in 50 μl sterile deionized water, and quantified for each density fraction. We determined the total numbers of bacterial 16S rRNA gene copies in each density fraction by quantitative PCR (qPCR) using a pan-bacterial broad-coverage quantitative PCR technique (26). All fractions were analyzed in triplicate in 10-μl reaction mixtures that included 1 μl of DNA template and 9 μl of reaction mixture containing 1.8 μM forward (5′-CCTACGGG**D**GGC**W**GCA-3′) and reverse (5′-GG ACTAC**HV**GGGT**M**TCTAATC-3′) primers (bold letters denote degenerate bases), 225 nM TaqMan minor groove-binding probe (6FAM [6-carboxyfluorescein] 5′-CAGCAGCCGCGGTA-3′ MGBNFQ), 1× Platinum quantitative PCR supermix-UDG (Life Technologies, Grand Island, NY), and molecular-grade water. Amplification and real-time fluorescence detection were performed on the 7900HT real-time PCR system (Applied Biosystems). We provide the qPCR data for all density fractions in the supplemental material.

Data analysis of total 16S rRNA gene copy numbers. Based on the qPCR data, we produced a conventional SIP density curve by graphing the proportion of total 16S rRNA gene copies as a function of density, an approach often used to visualize the effect of isotope incorporation on the distribution of densities across the bacterial assemblage, delineating heavy and light regions for sequencing (9–11). We also calculated the average DNA density for each tube as a weighted average of the density of each fraction in which 16S rRNA gene copies were detected, weighted by the proportional abundance of total 16S rRNA gene copies measured in that fraction for each tube. This provided an estimate of the average DNA density for each tube, enabling bootstrap testing of whether the addition of the isotope increased the density of DNA.

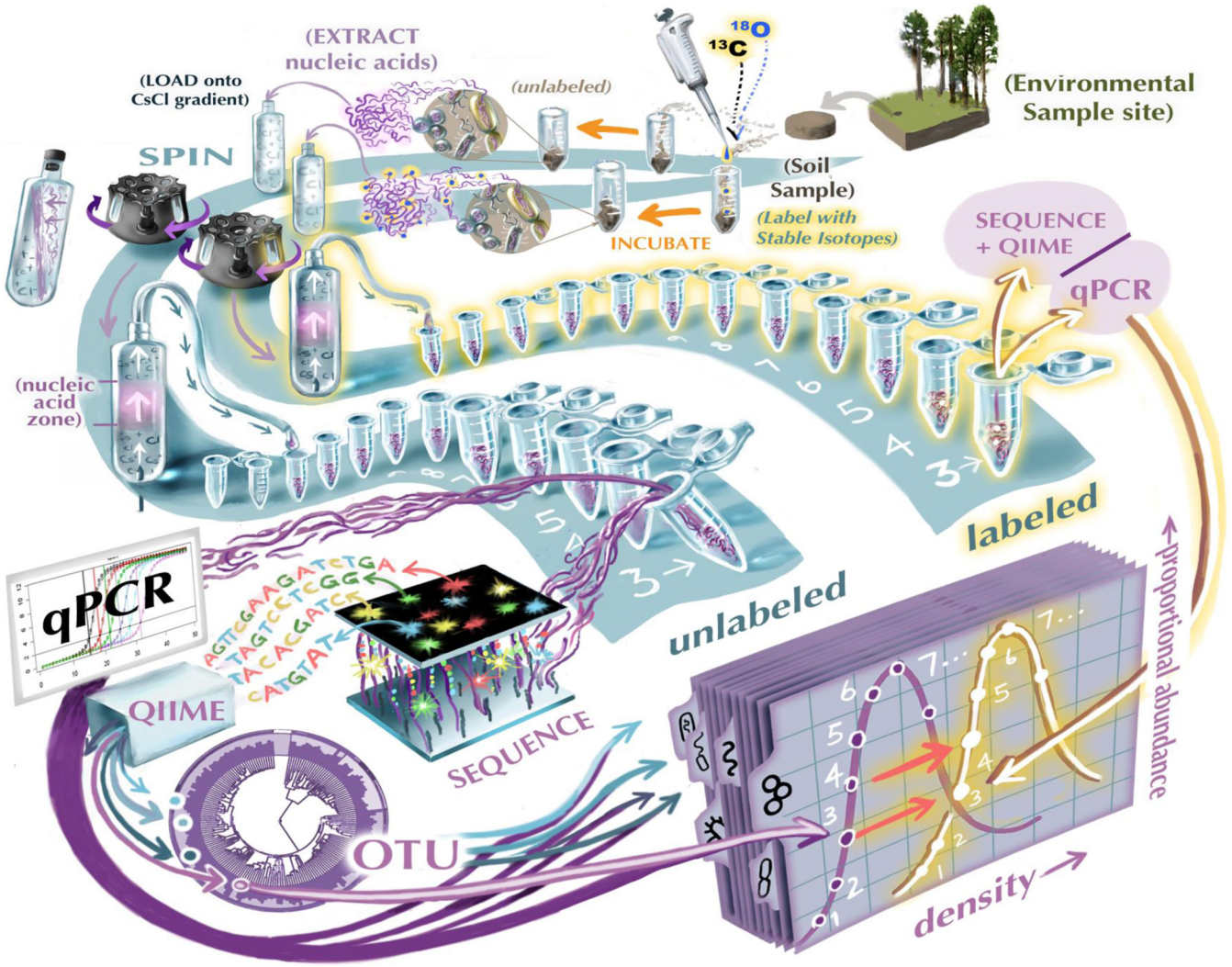

FIG 1 Conceptual model of the quantitative stable isotope probing technique, from sample collection to determining the density of 16S rRNA gene fractions for individual taxa and their corresponding values of atom % stable isotope composition. Note that, except for the addition of the stable isotope tracer at the beginning of the incubation, all steps are applied identically to both labeled and unlabeled samples. Artwork by Victor Leshyk.

Sequencing 16S rRNA genes. We sequenced the 16S rRNA gene in every density fraction that contained DNA (9 to 15 fractions per centrifuge tube) by dual-indexing amplicon-based sequencing on the Illumina MiSeq (Illumina, Inc., San Diego, CA, USA), using a previously published method (27). For each density fraction, the 16S rRNA gene V3-V4 hypervariable region was amplified in 25-μl reaction mixtures that included 5 μl of genomic DNA (gDNA) in a 20-μl reaction mixture containing 12.5 μl Phusion high-fidelity PCR master mix with HF buffer (New England BioLabs, Inc., Ipswich, MA, USA), 0.75 μl dimethyl sulfoxide (DMSO), 1.75 μl sterile water, and 0.2 μM each forward (5′-ACTCCTACGGGAG GCAGCAG-3′) and reverse (5′-GGACTAC**HV**GGGT**W**TC-TAAT-3′) primers, each concatenated to a linker sequence, a 12-bp barcode, and a heterogeneity spacer of 0 to 7 bp in size. The following thermocycling conditions were used: an initial denaturation at 98°C for 30s, followed by 30 cycles of denaturation at 98°C for 30s, annealing at 62°C for 30s, and amplification/extension at 72°C for 30s. The resultant amplicons were normalized and pooled using the SequelPrep normalization kit (Life Technologies, Carlsbad, CA, USA), purified using AMPure XT beads (Beckman Coulter Genomics, Danvers, MA, USA), and sequenced in combination with ~20% PhiX control library (version 3; Illumina) in 300-bp paired-end MiSeq runs.

Data analysis. Subsequent sequence processing and quality filtering were also performed as described in Fadrosh et al. (27). Each read was assigned to the original sample based on the 24-bp dual-index barcode formed by concatenating the 12-bp barcodes from each paired-end read. After trimming the primer sequences, the original V3-V4 amplicon was reconstituted by stitching the paired-end reads without preliminary quality filtering using FLASH (28), as FLASH includes error correction. We obtained 9,378,878 high-quality stitched reads that were subsequently processed at a median length of 410 bp.

The stitched reads were clustered using the uclust-based (29) open reference operational taxonomic unit (OTU) picking protocol (30) described in QIIME (version 1.8.0-dev) (31) against the Greengenes 13_8 reference database (32). Representative sequences for each OTU were chosen as the cluster centroid sequences. OTUs with representative sequences that could not be aligned with PyNAST and OTUs with a total count of less than 2 across all samples (i.e., singleton OTUs) were excluded from subsequent analyses, leaving a total of 76,710 OTUs composed of 9,127,632 reads.

All taxonomic assignments used throughout this study were generated by QIIME's uclust consensus taxonomy assigner (default parameters) (33) against the Greengenes 13_8 97% reference OTUs (32). The taxo-

TABLE 1 Definitions of indices, variables, and calculated quantities used in modeling atom fraction excess ^{18}O for each bacterial taxon

Parameter	Description
Indices	
i	Taxon
j	Replicate (or tube) within a treatment
k	Fraction (within a replicate)
I	No. of taxa
J	No. of replicates (within a treatment)
K	No. of fractions (within a replicate)
Variables	
f_{jk}	Total no. of 16S rRNA gene copies per μl (all taxa combined) in fraction k of replicate j (copies μl^{-1})
p_{ijk}	Proportion of the total no. of 16S rRNA gene copies per μl that are taxon i in fraction k of replicate j (unitless)
x_{jk}	Density of fraction k of replicate j (g cm^{-3})
Calculated quantities	
y_{ijk}	No. of 16S rRNA gene copies per μl of taxon i in fraction k of replicate j (copies μl^{-1})
y_{ij}	Total no. of 16S rRNA gene copies per μl of taxon i in replicate j (copies μl^{-1})
W_{ij}	Observed weighted avg density for taxon i in replicate j (g cm^{-3})
$W_{\mathrm{LAB}i}$	Mean observed weighted avg density for taxon i in the labeled treatment (mean across all replicates of the treatment with the heavy isotope) (g cm^{-3})
$W_{\mathrm{LIGHT}i}$	Mean observed weighted avg density for taxon i in the unlabeled (i.e., natural abundance) treatment (mean across all replicates in all treatments without heavy isotopes) (g cm^{-3})
G_i	Guanine-plus-cytosine content of taxon i (unitless)
$H_{\mathrm{CARBON}i}$	Avg no. of carbon atoms per DNA nucleotide for taxon i
$M_{\mathrm{LIGHT}i}$	Observed mol wt of the DNA fragment containing the 16S RNA gene for taxon i in the unlabeled (i.e., natural abundance) treatment (g mol^{-1})
$M_{\mathrm{HEAVYMAX}i}$	Theoretical mol wt of the DNA fragment containing the 16S RNA gene for taxon i assuming maximum labeling by the heavy isotope (g mol^{-1})
$M_{\mathrm{LAB}i}$	Observed mol wt of the DNA fragment containing the 16S RNA gene for taxon i in the labeled treatment (g mol^{-1})
Z_i	Difference in observed weighted avg densities of taxon i for the labeled and unlabeled treatments (g cm^{-3})
$A_{\mathrm{OXYGEN}i}$	Atom fraction excess of ^{18}O in the labeled vs unlabeled treatment for taxon i (unitless)
$A_{\mathrm{CARBON}i}$	Atom fraction excess of ^{13}C in the labeled vs unlabeled treatment for taxon i (unitless)

nomic abundances for each sample-taxon combination using the uclust consensus assigner were compared with taxonomic assignments made with the RDP classifier (confidence level of 0.5, as recommended in reference 34) using a nonparametric Pearson correlation test with 999 iterations. For each sample-taxon combination, taxonomic abundances were compared for the two assignment methods (i.e., using QIIME's compare_taxa_summaries.py script). The resulting P values were significant ($P < 0.001$) at all taxonomic levels, and the Pearson r values were high (>0.96) (see Table S1 in the supplemental material), indicating that the taxonomic profiles generated by the different methods were nearly identical. The analyses performed here focused on taxonomic classification to the level of genus, of which the uclust consensus assignment yielded a total of 790 genera. The genera included for analysis were the 379 that occurred in all replicate tubes; these were also the most abundant taxa, representing 99.531% of the total 16S rRNA gene copies across the data set. All QIIME commands used in this analysis are provided in the supplemental material.

Overview of quantitative taxon-specific isotope incorporation. In the following sections, we describe the calculations required to determine the isotopic composition of individual taxa after exposure to isotopically labeled substrates. In this approach, the taxon-specific density of DNA in the treatment with the isotopically labeled substrate is computed and compared to the density of DNA for the same taxon in the treatment with no added isotope tracer. For a particular element and isotope, the density of DNA will reach a maximum value when all atoms of that element in the DNA molecule are labeled with the isotope tracer. Smaller shifts in density reflect intermediate degrees of tracer incorporation; the scaling between density shift and isotope incorporation is linear after accounting for the effect of GC content on the elemental composition of DNA. The incorporation of the isotope tracer is expressed as atom fraction excess, which is the increase above the natural abundance isotopic composition and ranges from a minimum of 0 to a maximum of 1 minus the natural abundance background for a given isotope-element combination. Variables, calculated quantities, and indices are defined in Table 1.

Calculating taxon-specific changes in density. Taxon-specific changes in density caused by isotope incorporation were calculated as shown in equations 1 to 12 below. Calculations at the scale of individual density fractions (equation 1) and of individual replicate tubes (equations 2 and 3) were conducted for each density fraction and each tube independently. Other calculated quantities compared tubes with and without isotopes (equations 4 and 10 to 12), where we used means across replicates to estimate the mean difference and resampling with replacement (bootstrapping) to determine confidence intervals (CIs), as described below. In all cases, the independence of true replicates was preserved.

As described above, we determined the total number of 16S rRNA gene copies (f_k) using the universal 16S rRNA primer for qPCR of each fraction (k) in each replicate density gradient (j). Also as described above, we used sequencing to determine the proportional abundance of each taxon (i) within each density fraction (k), again for each replicate density gradient (j). This proportional abundance of each individual taxon within an individual density gradient from a particular replicate tube is abbreviated p_{ijk}. We calculated the total number of 16S rRNA gene copies per μl (y_{ijk}) for bacterial taxon i in density fraction k of replicate j as follows:

$$y_{ijk} = p_{ijk} \cdot f_{jk} \quad (1)$$

The total number of 16S rRNA gene copies (y_{ij}) for bacterial taxon i in replicate j is summed across all K density fractions as follows:

$$y_{ij} = \sum_{k=1}^{K} y_{ijk} \quad (2)$$

The density (W_{ij}) for bacterial taxon i of replicate j was computed as a weighted average, summing across all K density fractions the density (x_{jk}) of each individual fraction times the total number of 16S rRNA gene copies (y_{ijk}) in that fraction, expressed as a proportion of the total 16S rRNA gene copies (y_{ij}) for taxon i in replicate j, as follows:

$$W_{ij} = \sum_{k=1}^{K} x_{jk} \cdot \left(\frac{y_{ijk}}{y_{ij}} \right) \quad (3)$$

For a given taxon, we calculated the difference in density caused by isotope incorporation (Z_i) as follows:

$$Z_i = W_{\mathrm{LAB}i} - W_{\mathrm{LIGHT}i} \quad (4)$$

where $W_{\mathrm{LAB}i}$ is the mean, across all replicates, of the isotope-enriched treatment (labeled [LAB]; $n = 3$) and $W_{\mathrm{LIGHT}i}$ is the mean, across all replicates, of the unlabeled treatment (unlabeled [LIGHT]; $n = 6$). Because our experiment had multiple treatments without heavy isotopes, we included data from all replicate tubes in those unlabeled treatments (i.e., unlabeled treatments with and without added carbon; $n = 6$) to estimate the unlabeled average density ($W_{\mathrm{LIGHT}i}$) for each taxon i.

Calculating taxon-specific GC content and molecular weight. We calculated the GC content (G_i) of each bacterial taxon using the mean density for the unlabeled ($W_{\mathrm{LIGHT}i}$) treatments ($n = 6$). We derived the relationship between GC content and buoyant density using DNA from pure cultures of three microbial species with known and strongly differing GC contents (see below). For these cultures, the linear relationship between GC content (G_i, expressed as a proportion) and unlabeled buoyant density ($W_{\mathrm{LIGHT}i}$) on a CsCl gradient was as follows:

$$G_i = \frac{1}{0.083506} \cdot \left(W_{\mathrm{LIGHT}i} - 1.646057 \right) \quad (5)$$

This relationship differs from the established relationship between GC content and density (12). As noted above, our method of determining density relied on direct measurements of refraction on individual density fractions, as is the typical practice for SIP studies (25). It is possible that including DNA standards of known GC content in each ultracentrifuge would yield results more consistent with the established relationship. Practitioners should include specific measures to calibrate their laboratory techniques to this relationship.

The natural abundance molecular weight of DNA is a function of GC content, based on the atomic composition of the four DNA nucleotides. Single-stranded DNA made of pure adenine (A) and thymine (T) has an average molecular weight of 307.691 g mol^{-1}. The corresponding average molecular weight for DNA comprising only guanine (G) and cytosine (C) is 308.187 g mol^{-1}. When the GC content is known, the average molecular weight of a single strand of DNA can be calculated using the following equation:

$$M_{\mathrm{LIGHT}i} = 0.496 G_i + 307.691 \quad (6)$$

Percent change in molecular weight associated with isotope incorporation. There are 12 oxygen atoms per DNA nucleotide pair, regardless of GC content: 6 each for G and C, 7 for T, and 5 for A. These atoms contain ^{18}O at natural abundance, which we assume to be 0.002000429 atom fraction for ^{18}O (36). The maximum labeling is achieved when all oxygen atoms are replaced by ^{18}O. Therefore, given the molecular weight of each additional neutron (1.008665 g mol^{-1} [37]), the maximal increase in molecular weight (corresponding to 1 atom fraction ^{18}O, or 100% atom percent ^{18}O) is 12.07747 g mol^{-1}. The theoretical maximum molecular weight ($M_{\mathrm{HEAVYMAX}i}$) of fully ^{18}O-labeled DNA for taxon i is then calculated as follows:

$$M_{\mathrm{HEAVYMAX}i} = 12.07747 + M_{\mathrm{LIGHT}i} \quad (7)$$

In contrast, the number of carbon atoms per DNA nucleotide varies with GC content. There are 10 carbon atoms in G, A, and T but only 9 in C. The average number of carbon atoms per DNA nucleotide ($H_{\mathrm{CARBON}i}$) for taxon i can therefore be expressed as follows:

$$H_{\mathrm{CARBON}i} = -0.5 G_i + 10 \quad (8)$$

We assume these atoms are ^{13}C-labeled at natural abundance (0.01111233 atom fraction ^{13}C [36]). The maximal labeling is achieved when all carbon atoms are replaced by ^{13}C. Complete replacement of carbon atoms with ^{13}C increases the molecular weight by 9.974564 g mol^{-1} for G, A, and T and by 8.977107 g mol^{-1} for C. Using equation 8, the theoretical maximum molecular weight ($M_{\mathrm{HEAVYMAX}i}$) of fully ^{13}C-labeled DNA can be calculated as follows, with GC content (G_i) expressed as a proportion:

$$M_{\mathrm{HEAVYMAX}i} = -0.4987282 G_i + 9.974564 + M_{\mathrm{LIGHT}i} \quad (9)$$

Calculating isotope enrichment from density shifts. We calculated the proportional increase in density (Z_i) relative to the density of the unlabeled treatments ($W_{\mathrm{LIGHT}i}$) and calculated the molecular weight of DNA for taxon i in the labeled treatment ($M_{\mathrm{LAB}i}$) as follows:

$$M_{\mathrm{LAB}i} = \left(\frac{Z_i}{W_{\mathrm{LIGHT}i}} + 1 \right) \cdot M_{\mathrm{LIGHT}i} \quad (10)$$

The atom fraction excess of ^{18}O for taxon i ($A_{\mathrm{OXYGEN}i}$), accounting for the background fractional abundance of ^{18}O (0.002000429 [36]), is then calculated as follows:

$$A_{\mathrm{OXYGEN}i} = \frac{M_{\mathrm{LAB}i} - M_{\mathrm{LIGHT}i}}{M_{\mathrm{HEAVYMAX}i} - M_{\mathrm{LIGHT}i}} \cdot \left(1 - 0.002000429 \right) \quad (11)$$

We used the results from a pure culture study with *Escherichia coli*, grown using water with different levels of ^{18}O enrichment (natural abundance, 5, 25, 50, and 70% atom fraction ^{18}O; see below) to compare to the theoretical calculations of atom fraction excess ^{18}O derived above.

Similarly, the atom fraction excess ^{13}C for taxon i ($A_{\mathrm{CARBON}i}$), accounting for the background fractional abundance of ^{13}C (0.01111233 [36]), is calculated as follows:

$$A_{\mathrm{CARBON}i} = \frac{M_{\mathrm{LAB}i} - M_{\mathrm{LIGHT}i}}{M_{\mathrm{HEAVYMAX}i} - M_{\mathrm{LIGHT}i}} \cdot \left(1 - 0.01111233 \right) \quad (12)$$

Pure culture studies. To verify the predicted relationship between increased density and atom fraction excess, we conducted experiments with a pure *Escherichia coli* culture. The *E. coli* (strain HB101, GC content 50.8%) culture was shaken at 100 rpm for 8 h at 37°C in Luria-Bertani (LB) broth that was prepared with a mixture of natural abundance and [^{18}O]water to achieve five [^{18}O]enrichment levels (natural abundance, 5, 25, 50, and 70% atom fraction ^{18}O). Genomic DNA was extracted in triplicate using the PowerLyzer UltraClean microbial DNA isolation kit according to the manufacturer's instructions (Mo Bio Laboratories, Inc., Carlsbad, CA). We also grew pure cultures of two additional strains of bacteria selected for low GC content (*Staphylococcus epidermidis* ATCC 49461, 32.1%) and high GC content (*Micrococcus luteus* ATCC 49732, 73%). *S. epidermidis* was grown for 24 h on brain heart infusion agar at 37°C, and *M. luteus* was grown with LB agar at 23°C. These cultures were grown with substrates and water at natural abundance stable isotope composition.

For each culture, genomic DNA was extracted in triplicate. Approximately 800 ng of each DNA extract was used for isopycnic centrifugation, density quantification, and DNA isotope analysis. The ^{18}O composition of the *E. coli* DNA was determined with a PyroCube (Elementar Analysensysteme GmbH, Hanau, Germany) interfaced to a PDZ Europa 20-20 isotope ratio mass spectrometer (Sercon Ltd., Cheshire, United Kingdom) at the UC Davis Stable Isotope Facility (Davis, CA). Samples were prepared by diluting the *E. coli* DNA with natural abundance salmon sperm DNA to achieve enrichment levels below 100‰ δ^{18}O for isotope analysis. The densities of DNA from the cultures grown at natural abundance isotope composition were used to determine the relationship between the density of DNA and its GC content, yielding the relationship described in equation 5 ($r^2 = 0.912$; $P < 0.001$).

Statistical analysis. We used linear regression to examine the relationships between the [^{18}O]water composition of the growth medium and the ^{18}O composition of *E. coli* DNA, as well as between the ^{18}O composition of *E. coli* DNA and its density.

Following the equations above, we computed the difference in densities, Z_i, between treatments with and without isotope tracers and the corresponding values of isotope composition, A_{OXYGEN_i} and A_{CARBON_i}. Each calculated quantity was determined for each replicate sample. We then used bootstrap resampling (with replacement, 1,000 iterations) of replicates within each treatment to estimate taxon-specific 90% CIs for the change in density (equation 4) and the corresponding value of atom fraction excess isotope composition (equation 11 for oxygen and equation 12 for carbon). For each bootstrap iteration, three samples (with replacement) were drawn from the treatment with added isotope and six samples were drawn from the no-isotope controls. All calculations were performed in R (38).

Density fractionation separates organisms according to GC content (12), as well as isotope incorporation, so traditional SIP may be biased toward identifying high-GC-content organisms as growing or utilizing a substrate (39, 40). To test whether qSIP exhibited any such bias, we used density without isotope addition as a proxy for GC content and tested whether the densities of organisms identified as assimilating (90% CIs did not include 0 for A_{CARBON} or A_{OXYGEN}) differed in density from organisms where assimilation was not detected.

Our focus was on the magnitude of variation in Z_i, A_{OXYGEN}, and A_{CARBON}, because the goal of our work was to establish a means to discern from SIP experiments quantitative estimates of isotope tracer uptake. These values lie along a continuum from no uptake to complete isotope replacement, and our approach estimates the values and places confidence limits on those estimates. We did not use null hypothesis significance testing for assessing density shifts and isotope tracer uptake, because our priority was on estimation rather than determining statistical significance. For this reason, we selected bootstrap resampling rather than, for example, *t* tests or analyses of variance (ANOVAs). Parametric tests could of course be applied in future applications of this technique and may be appropriate, for example, for statistical comparisons of treatments postulated to alter isotope tracer uptake. In such cases, correcting for multiple comparisons may be appropriate, depending on the nature of the question and the balance between type I and type II error rates. We note that, in typical SIP experiments, an organism is considered to be growing or utilizing a substrate if it exhibits a change in relative abundance when comparing the heavy fraction of the labeled sample to the control (e.g., see reference 10) or comparing the heavy fraction to the light fraction (e.g., see reference 41), and yet, assessments of variation in these estimates are not typically presented. Our approach assesses both the quantitative values of isotope uptake and the variation associated with those estimates.

Accession number. All sequence data have been deposited at MG-RAST (35) under project accession number 14151.

RESULTS

In the pure culture experiments, the ^{18}O composition of *E. coli* DNA was strongly related to the ^{18}O composition of water in the growth medium, supporting the notion that oxygen from water is quantitatively incorporated into the DNA of growing organisms ($P < 0.001$; $r^2 = 0.976$) (Fig. 2A). The slope of the relationship, 0.334 ± 0.017 (mean $\pm$ standard deviation; $n = 15$), indicates that 33% of oxygen in *E. coli* DNA was derived from water. The shift in density of *E. coli* DNA with ^{18}O incorporation matched well the theoretical prediction of the model of isotope substitution in the DNA molecule (equations 10 and 11; Fig. 2B). These results confirm that ultracentrifugation in CsCl can serve as a quantitative mass separation procedure, resolving variations in isotope tracer incorporation into DNA. These results also support our model of the relationship between the density of nucleic acids and isotopic substitution in the DNA molecule.

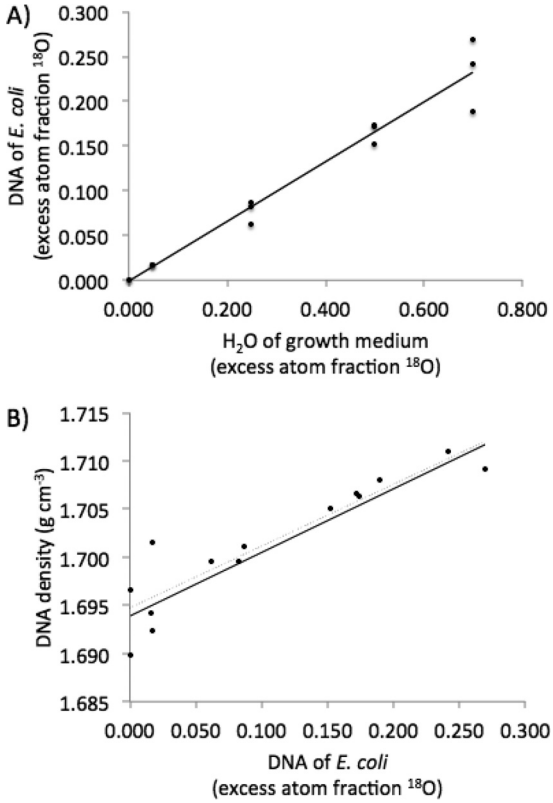

FIG 2 (A) ^{18}O composition of *E. coli* DNA as a function of the ^{18}O composition of water in the growth medium. Solid line is the regression ($^{18}O_{DNA} = 0.3339 \times {}^{18}O_{H2O} + 0.0004$; $n = 15$; $P < 0.001$; $R^2 = 0.976$). (B) Average density of *E. coli* DNA as a function of the ^{18}O composition of the DNA (density = $0.0644 \times$ atom fraction ^{18}O + 1.6946; $R^2 = 0.852$; $n = 15$).

In soil incubations, DNA density averaged across the entire community tended to increase in response to isotope addition (Fig. 3). The addition of [^{13}C]glucose (Fig. 3A) increased the density of DNA by 0.0043 g cm^{-3}, but the 90% CI for this increase overlapped zero (-0.002 to 0.0091 g cm^{-3}). The addition of ^{18}O-water (Fig. 3B) caused a similar increase in density, 0.0041 g cm^{-3}, but the 90% CI for this increase also overlapped zero, spanning -0.0011 to 0.0090 g cm^{-3}. The incubations receiving [^{18}O]water and supplemental glucose (natural abundance isotope composition) exhibited the largest increase in average DNA density, 0.0090 g cm^{-3}, and in this case, the 90% confidence limit did not overlap zero (0.0065 to 0.0125 g cm^{-3}). These comparisons estimate the change in density of DNA fragments encoding the 16S rRNA gene across all taxa considered together. Figure 3 also illustrates the density distributions often used in SIP experiments to visualize the qualitative cutoff between labeled and unlabeled regions suitable for sequencing.

Sequencing all fractions allowed analogous density distributions for individual taxa to be visualized. Figure 4 shows three taxa used to illustrate the concept, showing graphically the manner in which the density of labeled (W_{LAB_i}) and unlabeled (W_{LIGHT_i}) DNA is calculated for each taxon (equation 3). For example, the density of an unidentified genus in the family *Micrococcaceae* did not change with the addition of [^{18}O]water in the absence of sup-

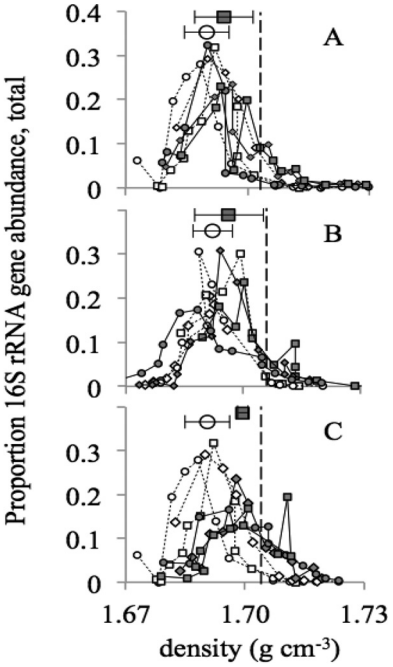

FIG 3 The relative levels of abundance of bacterial 16S rRNA genes, measured through quantitative PCR, as a function of density of DNA. Data for isotope treatments are shown with filled symbols, while data for natural abundance controls are shown with open symbols. Comparison of soil samples incubated with natural abundance glucose and [^{13}C]glucose (A), natural abundance water and [^{18}O]water (B), and natural abundance water plus natural abundance glucose and [^{18}O]water plus natural abundance glucose (C). The dotted lines represent the density that separates labeled from nonlabeled DNA in traditional SIP. The distribution of densities in each replicate tube yielded an estimate of the average density for that tube, indicated by the horizontal position of the large symbols and error bars at the top of each panel (bars show 90% CIs, with $n = 3$; the vertical position of these symbols does not convey meaning).

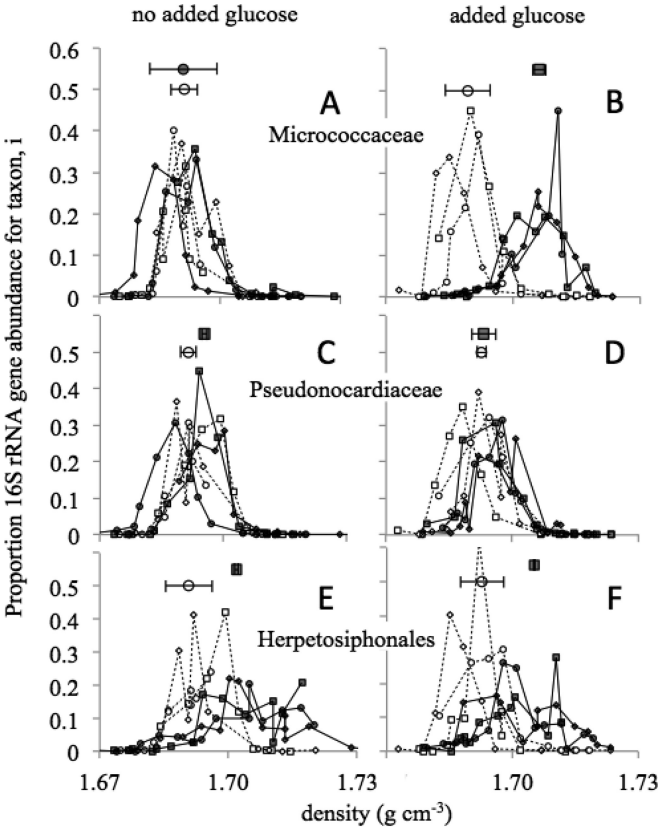

FIG 4 Frequency distribution of the 16S rRNA gene as a function of density of DNA for three bacterial taxa without added glucose (left) and with added (natural abundance δ^{13}C) glucose (right); the three different taxa included unidentified genera in the families *Micrococcaceae* (A and B) and *Pseudonocardiaceae* (C and D) and the genus *Herpetosiphonales* (E and F). Open symbols and dashed lines show the density distribution for the incubation where all substrates had natural abundance isotope composition, and filled symbols and solid lines show the distribution with [^{18}O]water. Different shapes represent individual replicates within a treatment combination. For each replicate, the area under the curve sums to 1. The distribution of densities for each taxon in each replicate yielded an estimate of the average density for that taxon, indicated by the horizontal position of the large symbols and error bars at the top of each panel (bars show 90% CIs, with $n = 3$; the vertical position of the large symbols does not convey meaning).

plemental glucose. For this taxon, the shift in density (Z) due to ^{18}O incorporation was -0.0002 g cm^{-3}, with the 90% CI spanning -0.0046 to 0.0049 g cm^{-3} (Fig. 4A). The shift in density due to ^{18}O incorporation increased when unlabeled glucose was also added ($Z = 0.0169$ g cm^{-3}, 90% CI of 0.0146 to 0.0194 g cm^{-3}) (Fig. 4B). This bacterial taxon, therefore, did not incorporate the ^{18}O tracer in unamended soil but did synthesize new DNA using ^{18}O derived from H_2O in response to glucose addition. The DNA of an unidentified genus in the family *Pseudonocardiaceae* similarly exhibited no change in density in the absence of supplemental glucose ($Z = 0.0005$ g cm^{-3}, 90% CI of -0.0033 to 0.0045 g cm^{-3}) and exhibited only a slight increase in response to the addition of glucose ($Z = 0.0040$ g cm^{-3}, 90% CI of 0.0015 to 0.0070 g cm^{-3}) (Fig. 4C and D). In contrast, the density of DNA in a member of the genus *Herpetosiphonales* increased in soil without any supplemental glucose ($Z = 0.0124$ g cm^{-3}, 90% CI of 0.0105 to 0.0143 g cm^{-3}) (Fig. 4E), but the density did not increase further in response to the addition of glucose ($Z = 0.0110$ g cm^{-3}, 90% CI of 0.0088 to 0.0133 g cm^{-3}) (Fig. 4F). These results show that, by dividing the density gradient into multiple fractions and sequencing each separately, one can determine changes in the density of DNA for individual taxa caused by the assimilation of stable isotope tracers.

The taxon-specific shifts in average density associated with incorporation of the heavy isotope (Fig. 5) translate directly to quantitative variation in isotope composition, expressed here as atom fraction excess ^{18}O (A_{OXYGEN}) (Fig. 5, left and middle) and ^{13}C (A_{CARBON}) (Fig. 5, right). The detection limit for a shift in density is the median change in density required to shift the lower bound of the bootstrapped 90% confidence limit above zero. As constrained by our sampling design, these values were 0.0037 g cm^{-3} for ^{18}O and 0.0044 g cm^{-3} for ^{13}C, changes that correspond to 0.056 atom fraction excess ^{18}O and 0.081 atom fraction excess ^{13}C. No taxon exhibited a detectable decline in density in response to isotope addition (i.e., a negative mean density shift with a confidence interval that did not include zero).

More than half of the bacterial genera (209 genera) did not exhibit any detectable excess ^{18}O enrichment under control conditions without added glucose; in other words, the lower bounds of the confidence intervals for these genera overlapped zero (Fig. 5, left). Of the 170 taxa that did exhibit detectable ^{18}O enrichment without added glucose, the corresponding values of atom fraction excess ^{18}O ranged from 0.047 (90% CI of 0.001 to 0.100) in a

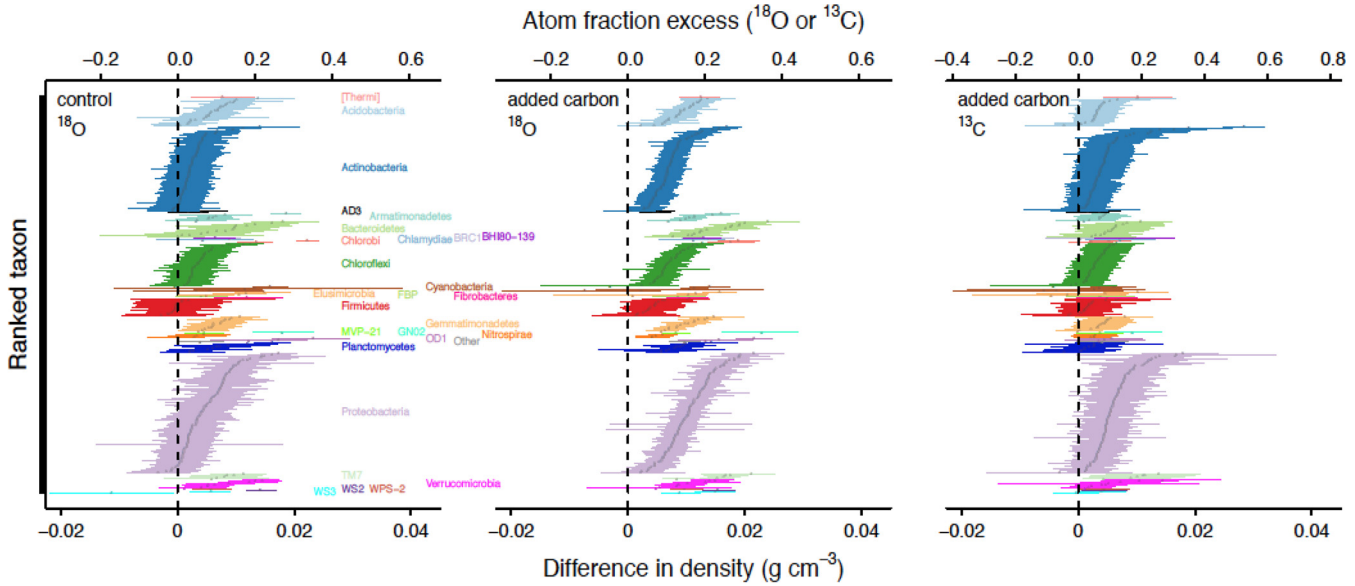

FIG 5 Taxon-specific shifts in average density of DNA (g cm^{-3}, bottom horizontal axis) and corresponding atom fraction excess of ^{18}O or ^{13}C (top horizontal axis) between incubations with enriched and natural abundance substrates. Changes in DNA density were caused by ^{18}O incorporation from water without (left) or with (middle) added natural abundance glucose or by ^{13}C incorporation from added ^{13}C-labeled glucose (right). Bars show bootstrapped medians and 90% CIs.

member of the genus *Lentzea* to 0.354 (90% CI of 0.248 to 0.449) in an unidentified representative of the candidate bacterial phylum *OD1*. With added glucose, 351 of the 379 taxa exhibited positive atom fraction excess ^{18}O (90% CIs did not overlap zero), averaging 0.147 (Fig. 5, middle), with a minimum of 0.036 (90% CI of 0.004 to 0.064) in an unidentified genus of the family *Ktedonobacteraceae* and a maximum of 0.365 (90% CI of 0.282 to 0.449) in an unidentified genus within the class *AT12OctB3* of the phylum *Bacteroidetes*. The bacterial taxa in this soil varied in atom fraction excess ^{18}O under control conditions and in response to added glucose (Fig. 5, left and middle). Atom fraction excess ^{13}C reflects direct assimilation of C from the added glucose (Fig. 5, right), and it ranged from no detectable enrichment among 215 of the 379 genera to over half of the carbon atoms comprising ^{13}C in the DNA of a member of the *Micrococcaceae* (0.525, 90% CI of 0.458 to 0.592).

GC bias. There was no evidence of GC bias in qSIP. There were negligible differences in densities between organisms exhibiting tracer assimilation and those not exhibiting tracer assimilation (Table 2). The inferred GC contents averaged 52.3% (90% CI of 44.6 to 57.3) for organisms exhibiting tracer assimilation, very close to the average of 52.8% inferred GC content for taxa for which assimilation was not detected (90% CI of 45.1 to 58.2).

TABLE 2 Density of DNA for taxa exhibiting or not exhibiting tracer assimilation in the three tracer experiments

Tracer	Mean DNA density (g cm^{-3}) ± SD for taxa that:	
	Assimilated tracer	Did not assimilate tracer
[^{18}O]water	1.6905 ± 0.0031	1.6912 ± 0.0033
[^{18}O]water with glucose	1.6896 ± 0.0033	1.6894 ± 0.0045
[^{13}C]glucose	1.6890 ± 0.0030	1.6900 ± 0.0036

Soil incubations: multiple-element quantitative stable isotope probing. There was a strong positive relationship between increased atom fraction excess ^{18}O in response to the addition of glucose and the direct utilization of glucose-derived C (atom fraction excess ^{13}C; $r^2 = 0.51$, $P < 0.001$) (Fig. 6). The expected relationship (Fig. 6, solid line) reflects the case where glucose is the sole C source, and thus, there should be a 0.33 atom fraction excess increase in ^{18}O for each 1 atom fraction excess increase in ^{13}C, based on our finding that 33% of the oxygen molecules in DNA are derived from water (Fig. 2). For many taxa, the increase in atom fraction excess ^{18}O in response to added glucose exceeded the expected amount (Fig. 6, solid line).

DISCUSSION

We demonstrate that stable isotope probing of bacterial assemblages in natural environments can yield quantitative information about the assimilation of isotope tracers into bacterial DNA with fine taxonomic resolution. This work establishes a framework for coupling quantitative interpretation of stable isotope tracer experiments with microbial diversity, a coupling essential for understanding how to represent microbial diversity in biogeochemical models.

The shifts in density we could detect using qSIP (0.0034 to 0.0042 g cm^{-3}) (Fig. 5) are nearly an order of magnitude smaller than those typically used to resolve the assimilation of stable isotopes into newly synthesized DNA using conventional SIP, in which light and heavy density fractions often differ by 0.03 g cm^{-3} (14, 42) or more (13, 25, 43). For ^{13}C, the minimum required change in density for SIP has been estimated to be 0.01 g cm^{-3}, corresponding to 0.2 atom fraction excess (7). The approach presented here achieves higher resolution by accounting for taxonomic differences in the density of DNA caused by natural variation in GC content. It may be possible to improve the resolution we achieved. We collected fractions in discrete density increments

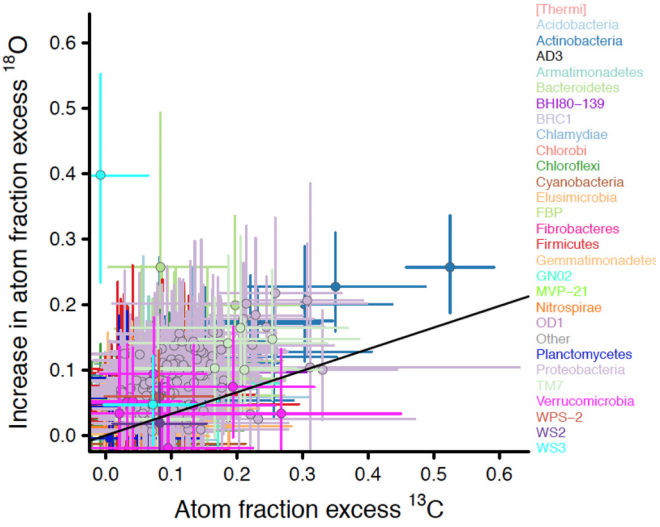

FIG 6 Atom fraction ^{13}C with added [^{13}C]glucose and the shift in atom fraction ^{18}O caused by added natural abundance glucose across groups of bacteria. The solid black line represents the expected relationship if organisms derived 100% of their carbon from the added glucose and 33% of their oxygen from [^{18}O]water. The differences between the solid line and points falling above it are due to the indirect effect of added glucose on the utilization of other carbon substrates, reflecting the difference between the total growth stimulation caused by glucose addition and the stimulation based on direct reliance on the added glucose. Points and error bars show means and standard errors of the means ($n = 3$).

of 0.0036 g cm^{-3} (average difference in density between adjacent fractions), setting a limit on the changes in density we could detect. This difference in density between the adjacent fractions we collected is comparable to the density shifts of bacterial taxa that we could resolve: the mean density shift required for the lower confidence limit to exceed zero was, on average, 0.0034 g cm^{-3} for ^{18}O and 0.0042 g cm^{-3} for ^{13}C. Thus, it is possible that separation of the nucleic acids into finer density fractions will afford higher precision in the estimates of stable isotope composition. Furthermore, our sample size was quite low; higher replication would achieve finer resolution. Nevertheless, the finding that no taxon exhibited a detectable decline in density in response to isotope addition is encouraging. Such a result would be illogical because isotope tracer uptake cannot be negative, but it could arise from large random variation (natural and measurement error) and low sample size. The absence here of such negative confidence intervals indicates that our bootstrapping application to qSIP is not particularly subject to false-positive inference.

The resolution achieved by sequencing individual density fractions, though an improvement over traditional SIP, is still very coarse compared to the resolution achieved with isotope ratio mass spectrometry. The detection of differences between taxa with quantitative stable isotope probing (~0.05 atom fraction excess) is 4 orders of magnitude less precise than that achieved with gas isotope ratio analysis of bulk organic matter in continuous flow, where differences of 0.000005 atom fraction excess or better (<0.5‰) can be resolved (44). Isopycnic centrifugation to quantify isotope composition is also less precise than compound-specific analysis of biomarkers, for example, of ^{13}C in fatty acids, where resolution of 0.00002 atom fraction excess (or 2‰) is typical (45–47). Coupling stable isotope tracing with nanoscale secondary ion mass spectrometry (Nano-SIMS) and microarrays, a coupling called Chip-SIP (48), can resolve 0.005 atom fraction excess for ^{15}N and 0.001 for ^{13}C (49), considerably more precise than qSIP.

qSIP has advantages over these other techniques in taxonomic resolution. For compound-specific biomarkers, specific fatty acids serve as biomarkers for up to a dozen groups of microorganisms, which is much coarser taxonomic resolution than that afforded by qSIP. Chip-SIP requires nucleic acid probes, necessitating *a priori* decisions as to what sequences to collect for isotopic analysis and the preparation of microarrays implanted with those sequences prior to the addition of the isotope. For this reason, in Chip-SIP, the taxonomic resolution in the isotope fluxes is influenced by information gathered without knowledge of which taxa are biogeochemically important. One advantage of qSIP is that sequencing occurs after isotope enrichment, enabling quantitative exploration of the biodiversity involved in biogeochemistry without having to decide *a priori* where to focus. Furthermore, the taxonomic resolution possible with a microarray is limited by probe specificity and fidelity, whereas the resolution afforded by qSIP is very high, equivalent to the resolution of the sequencing technology applied to the density fractions. Chip-SIP also requires access to Nano-SIMS, which is expensive and technically challenging, limiting its wide adoption in the field.

Other approaches used to link element fluxes to microbial taxa are limited to target organisms, such as fluorescent *in situ* hybridization (FISH) coupled with SIMS (50) or halogen *in situ* hybridization-SIMS (51). Bromodeoxyuridine (BrdU) uptake has been proposed as a universal technique for identifying growing organisms (52) and their responses to environmental perturbations (53). However, there is up to 10-fold variation among taxa in the conversion between BrdU uptake and growth that is unrelated to taxonomic affiliation, a bias calling into question the quantitative universality of this technique (54). Compared to these other techniques, qSIP can assess quantitatively the entire microbial assemblage at fine taxonomic resolution, a solid foundation for exploring quantitatively the relationships between microbial biodiversity and the biogeochemistry known to be microbial.

Our finding that many bacterial taxa did not exhibit any increase in ^{18}O content under control conditions (Fig. 5, left) is consistent with the notion that a portion of the soil microbial biomass is not growing and may be metabolically inactive (55). The increase in atom fraction ^{18}O and ^{13}C with added glucose indicates that the addition of glucose stimulates bacterial growth, not just respiration. The breadth of taxa that exhibited a positive response to glucose addition is consistent with glucose being a widely utilized substrate (56), though there are two other possible mechanisms. First, over the 7-day duration of the incubation period, glucose was assimilated by cells that then died, releasing labeled cellular constituents that were then available to the rest of the microbial community (57). We cannot distinguish between direct utilization of the added glucose and utilization of labeled cellular constituents produced by another organism. This applies equally to the ^{18}O-labeled and ^{13}C-labeled assemblages. Second, [^{18}O]water is a universal tracer for DNA synthesis, not necessarily tied to any particular carbon source (58, 59). The observed increase in atom fraction excess ^{18}O includes growth stimulation caused by the carbon contained in the added glucose, along with the growth stimulation caused by increased rates of utilization of other carbon sources. In contrast, atom fraction excess ^{13}C in

response to [^{13}C]glucose addition traces the incorporation of carbon atoms from glucose (or derived from glucose via other metabolites, as discussed above) into newly synthesized DNA (Fig. 5, right). This is expected, because the addition of glucose stimulates growth and DNA synthesis (60, 61). In summary, the effect of added glucose was apparent as (i) an overall stimulation of growth, independent of the specific carbon substrate, and (i) a stimulation of growth that relied directly on glucose-derived carbon.

The combination of ^{18}O and ^{13}C tracers enabled quantitative partitioning of these direct and indirect effects, based on the deviation in the data from the expected relationship between ^{18}O and ^{13}C enrichment for organisms utilizing glucose as a sole carbon source (Fig. 6, solid line). One explanation for this deviation is that most taxa derive more than 33% of the oxygen in DNA from environmental water. Quantitative variation in the contribution of water to oxygen in DNA could occur, for example, due to the variation in the oxidation state of the carbon substrate (e.g., lipids versus carbohydrates), though to our knowledge, this variation is not known. Given the universality of the mechanism of DNA replication, it is unlikely that taxa vary widely in the contribution of water to oxygen, at least when grown on a common substrate.

A more parsimonious explanation of the deviation we observed is that it represents the utilization of C sources other than glucose for growth. In other words, the added glucose stimulated the utilization of native soil C as a growth substrate. This points to the potential for quantitative stable isotope probing to test hypotheses regarding microbial diversity in the commonly observed phenomenon where the addition of simple C substrates to soil alters the mineralization of native soil C (16). This so-called priming effect is common and quantitatively significant (16) but remains mechanistically inscrutable. In past priming studies employing ^{13}C-SIP, some components of the microbial community were found to utilize as growth substrates the ^{13}C-labeled compounds added to initiate priming, though inferences about the organisms responsible for priming—i.e., degrading native soil organic matter—were weak, because no independent marker could validate their activity (62–64). Combining isotope tracers (using both ^{13}C and ^{18}O) can help by distinguishing microorganisms that respond to the original substrate pulse from those that respond indirectly by degrading soil organic matter (11), an approach useful for testing hypotheses about which groups of microorganisms contribute to priming. qSIP advances this one step further, by enabling quantitative comparisons of microorganisms' utilization of the added substrate and of soil organic matter for growth. Future analyses combining qSIP with system-level C fluxes would support stronger inferences about the role of specific microorganisms in the priming effect. The analysis presented here suggests that some microorganisms respond to glucose addition by enhancing their rates of utilization of native soil carbon, enabling additional biosynthesis (Fig. 6). More generally, the taxonomic diversity of responses we observed highlights the potential for this technique to provide insight into the population and community ecology behind biogeochemical phenomena involving such indirect effects (e.g., see references 16 and 17).

Quantifying isotope composition is the first step in determining the rate of substrate utilization in isotope tracer experiments and the foundation for comparing rates of substrate utilization and element fluxes among different taxa in intact microbial communities. This work advances a quantitative approach to stable isotope probing in order to elucidate taxon-specific processes that drive element cycling in intact communities, bringing to microbial ecology the power of stable isotopes to quantify rates of element fluxes into and through organisms (65, 66). Like Chip-SIP (48, 67), qSIP provides a means to quantify the ecology of organisms about which we know little more than the genetic fragment used to identify their unique place on the tree of life. These approaches lay the groundwork for a quantitative understanding of microbial ecosystems, including the types of ecological interactions previously described among macroorganisms that influence ecosystem processes. Quantitative stable isotope probing adds to the suite of tools that facilitate the interpretation of stable isotope tracer experiments in microbial communities, probing the quantitative significance of microbial taxa for biogeochemical cycles in nature.

ACKNOWLEDGMENTS

This research was supported by grants from the National Science Foundation (EAR-1124078 and DEB-1321792) and the Department of Energy's Biological Systems Science Division, Program in Genomic Science.

REFERENCES

1. **Jenny H.** 1941. Factors of soil formation: a system of quantitative pedology. Dover Publications, New York, NY.
2. **Vitousek PM.** 1990. Biological invasions and ecosystem processes—towards an integration of population and ecosystem studies. Oikos **57:**7–13. http://dx.doi.org/10.2307/3565731.
3. **Pace NR.** 1997. A molecular view of microbial diversity and the biosphere. Science **276:**734–740. http://dx.doi.org/10.1126/science.276.5313.734.
4. **Amann RI, Ludwig W, Schleifer KH.** 1995. Phylogenetic identification and in situ detection of individual microbial cells without cultivation. Microbiol Rev **59:**143–169.
5. **Muyzer G, Dewaal EC, Uitterlinden AG.** 1993. Profiling of complex microbial populations by denaturing gradient gel-electrophoresis analysis of polymerase chain reaction-amplified genes coding for 16S rRNA. Appl Environ Microbiol **59:**695–700.
6. **Roesch LF, Fulthorpe RR, Riva A, Casella G, Hadwin AKM, Kent AD, Daroub SH, Camargo FAO, Farmerie WG, Triplett EW.** 2007. Pyrosequencing enumerates and contrasts soil microbial diversity. ISME J **1:**283–290. http://dx.doi.org/10.1038/ismej.2007.53.
7. **Radajewski S, Ineson P, Parekh NR, Murrell JC.** 2000. Stable-isotope probing as a tool in microbial ecology. Nature **403:**646–649. http://dx.doi.org/10.1038/35001054.
8. **Hutchens E, Radajewski S, Dumont MG, McDonald IR, Murrell JC.** 2004. Analysis of methanotrophic bacteria in Movile Cave by stable isotope probing. Environ Microbiol **6:**111–120. http://dx.doi.org/10.1046/j.1462-2920.2003.00543.x.
9. **Sharp CE, Martinez-Lorenzo A, Brady AL, Grasby SE, Dunfield PF.** 2014. Methanotrophic bacteria in warm geothermal spring sediments identified using stable-isotope probing. FEMS Microbiol Ecol **90:**92–102. http://dx.doi.org/10.1111/1574-6941.12375.
10. **Schwartz E, Van Horn DJ, Buelow HN, Okie JG, Gooseff MN, Barrett JE, Takacs-Vesbach CD.** 2014. Characterization of growing bacterial populations in McMurdo Dry Valley soils through stable isotope probing with O-18-water. FEMS Microbiol Ecol **89:**415–425. http://dx.doi.org/10.1111/1574-6941.12349.
11. **Mau RL, Liu CM, Aziz M, Schwartz E, Dijkstra P, Marks JC, Price LB, Keim P, Hungate BA.** 2015. Linking soil bacterial diversity and soil carbon stability. ISME J **9:**1477–1480. http://dx.doi.org/10.1038/ismej.2014.205.
12. **Schildkraut CL.** 1962. Determination of base composition of deoxyribonucleic acid from its buoyant denstiy in CsCl. J Mol Biol **4:**430–443. http://dx.doi.org/10.1016/S0022-2836(62)80100-4.
13. **Schmidt O, Horn MA, Kolb S, Drake HL.** 2015. Temperature impacts differentially on the methanogenic food web of cellulose-supplemented peatland soil. Environ Microbiol **17:**720–734. http://dx.doi.org/10.1111/1462-2920.12507.
14. **Aanderud ZT, Jones SE, Fierer N, Lennon JT.** 2015. Resuscitation of the rare biosphere contributes to pulses of ecosystem activity. Front Microbiol **6:**24. http://dx.doi.org/10.3389/fmicb.2015.00024.

15. **Jayamani I, Cupples AM.** 2015. Stable isotope probing and high-throughput sequencing implicate Xanthomonadaceae and Rhodocyclaceae in ethylbenzene degradation. Environ Eng Sci **32:**240–249. http://dx.doi.org/10.1089/ees.2014.0456.
16. **Kuzyakov Y, Friedel JK, Stahr K.** 2000. Review of mechanisms and quantification of priming effects. Soil Biol Biochem **32:**1485–1498. http://dx.doi.org/10.1016/S0038-0717(00)00084-5.
17. **Bingeman CW, Varner JE, Martin WP.** 1953. The effect of the addition of organic materials on the decomposition of an organic soil. Soil Sci Soc Am J **17:**34–38. http://dx.doi.org/10.2136/sssaj1953.03615995001700010008x.
18. **Lohnis F.** 1926. Nitrogen availability of green manures. Soil Sci Soc Am J **22:**171–177.
19. **Broadbent FE.** 1948. Nitrogen release and carbon loss from soil organic matter during decomposition of added plant residues. Soil Sci Soc Am Proc **12:**246–249. http://dx.doi.org/10.2136/sssaj1948.036159950012000C0057x.
20. **Broadbent FE, Bartholomew WV.** 1948. The effect of quantity of plant material added to soil on its rate of decomposition. Soil Sci Soc Am Proc **13:**271–274. http://dx.doi.org/10.2136/sssaj1949.036159950013000C0048x.
21. **Kuzyakov Y.** 2002. Factors affecting rhizosphere priming effects. J Plant Nutr Soil Sci **165:**382–396. http://dx.doi.org/10.1002/1522-2624(200208)165:4<382::AID-JPLN382>3.0.CO;2-#.
22. **Blagodatskaya E, Kuzyakov Y.** 2008. Mechanisms of real and apparent priming effects and their dependence on soil microbial biomass and community structure: critical review. Biol Fertil Soils **45:**115–131. http://dx.doi.org/10.1007/s00374-008-0334-y.
23. **Hungate BA, Mau RL, Schwartz E, Caporaso JG, Dijkstra P, van Gestel N, Koch BJ, Liu CM, McHugh TA, Marks JC, Morrissey E, Price LB.** 2015. Quantitative microbial ecology through stable isotope probing. PeerJ PrePrints **3:**e1575. http://dx.doi.org/10.7287/peerj.preprints.1282v1.
24. **Mesbah NM, Whitman WB, Mesbah M.** 2011. Determination of the G plus C content of prokaryotes. Methods Microbiol **38:**299–324. http://dx.doi.org/10.1016/B978-0-12-387730-7.00014-0.
25. **Neufeld JD, Vohra J, Dumont MG, Lueders T, Manefield M, Friedrich MW, Murrell JC.** 2007. DNA stable-isotope probing. Nat Protoc **2:**860–866. http://dx.doi.org/10.1038/nprot.2007.109.
26. **Liu CM, Aziz M, Kachur S, Hsueh P-R, Huang Y-T, Keim P, Price LB.** 2012. BactQuant: an enhanced broad-coverage bacterial quantitative real-time PCR assay. BMC Microbiol **12:**56. http://dx.doi.org/10.1186/1471-2180-12-56.
27. **Fadrosh DW, Ma B, Gajer P, Sengamalay N, Ott S, Brotman RM, Ravel J.** 2014. An improved dual-indexing approach for multiplexed 16S rRNA gene sequencing on the Illumina MiSeq platform. Microbiome **2:**6. http://dx.doi.org/10.1186/2049-2618-2-6.
28. **Magoc T, Salzberg SL.** 2011. FLASH: fast length adjustment of short reads to improve genome assemblies. Bioinformatics **27:**2957–2963. http://dx.doi.org/10.1093/bioinformatics/btr507.
29. **Edgar RC.** 2010. Search and clustering orders of magnitude faster than BLAST. Bioinformatics **26:**2460–2461. http://dx.doi.org/10.1093/bioinformatics/btq461.
30. **Rideout JR, He Y, Navas-Molina JA, Walters WA, Ursell LK, Gibbons SM, Chase J, McDonald D, Gonzalez A, Robbins-Pianka A, Clemente JC, Gilbert JA, Huse SM, Zhou HW, Knight R, Caporaso JG.** 2014. Subsampled open-reference clustering creates consistent, comprehensive OTU definitions and scales to billions of sequences. PeerJ **2:**e545. http://dx.doi.org/10.7717/peerj.545.
31. **Caporaso JG, Kuczynski J, Stombaugh J, Bittinger K, Bushman FD, Costello EK, Fierer N, Pena AG, Goodrich JK, Gordon JI, Huttley GA, Kelley ST, Knights D, Koenig JE, Ley RE, Lozupone CA, McDonald D, Muegge BD, Pirrung M, Reeder J, Sevinsky JR, Turnbaugh PJ, Walters WA, Widmann J, Yatsunenko T, Zaneveld J, Knight R.** 2010. QIIME allows analysis of high-throughput community sequencing data. Nat Methods **7:**335–336. http://dx.doi.org/10.1038/nmeth.f.303.
32. **McDonald D, Price MN, Goodrich J, Nawrocki EP, DeSantis TZ, Probst A, Andersen GL, Knight R, Hugenholtz P.** 2012. An improved Greengenes taxonomy with explicit ranks for ecological and evolutionary analyses of bacteria and archaea. ISME J **6:**610–618. http://dx.doi.org/10.1038/ismej.2011.139.
33. **Bokulich NA, Rideout JR, Kopylova E, Bolyen E, Patnode J, Ellett Z, McDonald D, Wolfe B, Maurice CF, Dutton RJ, Turnbaugh PJ, Knight R, Caporaso JG.** 2015. A standardized, extensible framework for optimizing classification improves marker-gene taxonomic assignments. PeerJ PrePrints **3:**e1502. http://dx.doi.org/10.7287/peerj.preprints.934v2.
34. **Claesson MJ, O'Sullivan O, Wang Q, Nikkila J, Marchesi JR, Smidt H, de Vos WM, Ross RP, O'Toole PW.** 2009. Comparative analysis of pyrosequencing and a phylogenetic microarray for exploring microbial community structures in the human distal intestine. PLoS One **4:**e6669. http://dx.doi.org/10.1371/journal.pone.0006669.
35. **Meyer F, Paarmann D, D'Souza M, Olson R, Glass EM, Kubal M, Paczian T, Rodriguez A, Stevens R, Wilke A, Wilkening J, Edwards RA.** 2008. The metagenomics RAST server—a public resource for the automatic phylogenetic and functional analysis of metagenomes. BMC Bioinform **9:**386. http://dx.doi.org/10.1186/1471-2105-9-386.
36. **Coplen TB.** 1996. Atomic weights of the elements. Pure Appl Chem **68:**2339–2359.
37. **NIST.** 2015. The NIST reference on constants, units, and uncertainty. National Institute of Standards and Technology. http://physics.nist.gov/cuu/index.html. Accessed 2 July 2015.
38. **R Development Core Team.** 2014. R: a language and environment for statistical computing. R Foundation for Statistical Computing. http://www.R-project.org/.
39. **Rangel-Castro JI, Killham K, Ostle N, Nicol GW, Anderson IC, Scrimgeour CM, Ineson P, Meharg A, Prosser JI.** 2005. Stable isotope probing analysis of the influence of liming on root exudate utilization by soil microorganisms. Environ Microbiol **7:**828–838. http://dx.doi.org/10.1111/j.1462-2920.2005.00756.x.
40. **Kovatcheva-Datchary P, Egert M, Maathuis A, Rajilic-Stojanovic M, de Graaf AA, Smidt H, de Vos WM, Venema K.** 2009. Linking phylogenetic identities of bacteria to starch fermentation in an in vitro model of the large intestine by RNA-based stable isotope probing. Environ Microbiol **11:**914–926. http://dx.doi.org/10.1111/j.1462-2920.2008.01815.x.
41. **Darjany LE, Whitcraft CR, Dillon JG.** 2014. Lignocellulose-responsive bacteria in a southern California salt marsh identified by stable isotope probing. Front Microbiol **5:**263. http://dx.doi.org/10.3389/fmicb.2014.00263.
42. **Hu HW, Macdonald CA, Trivedi P, Holmes B, Bodrossy L, He JZ, Singh BK.** 2015. Water addition regulates the metabolic activity of ammonia oxidizers responding to environmental perturbations in dry subhumid ecosystems. Environ Microbiol **17:**444–461. http://dx.doi.org/10.1111/1462-2920.12481.
43. **Jiang XJ, Hou XY, Zhou X, Xin XP, Wright A, Ji ZJ.** 2015. pH regulates key players of nitrification in paddy soils. Soil Biol Biochem **81:**9–16. http://dx.doi.org/10.1016/j.soilbio.2014.10.025.
44. **Brenna JT, Corso TN, Tobias HJ, Caimi RJ.** 1997. High-precision continuous-flow isotope ratio mass spectrometry. Mass Spectrom Rev **16:**227–258. http://dx.doi.org/10.1002/(SICI)1098-2787(1997)16:53.3.CO;2-U.
45. **Amelung W, Brodowski S, Sandhage-Hofmann A, Bol R.** 2008. Combining biomarker with stable isotope analysis for assessing the transformation and turnover of soil organic matter. Adv Agron **100:**155–250. http://dx.doi.org/10.1016/S0065-2113(08)00606-8.
46. **Kramer C, Gleixner G.** 2008. Soil organic matter in soil depth profiles: distinct carbon preferences of microbial groups during carbon transformation. Soil Biol Biochem **40:**425–433. http://dx.doi.org/10.1016/j.soilbio.2007.09.016.
47. **Treonis AM, Ostle NJ, Stott AW, Primrose R, Grayston SJ, Ineson P.** 2004. Identification of groups of metabolically-active rhizosphere microorganisms by stable isotope probing of PLFAs. Soil Biol Biochem **36:**533–537. http://dx.doi.org/10.1016/j.soilbio.2003.10.015.
48. **Pett-Ridge J, Weber PK.** 2012. NanoSIP: NanoSIMS applications for microbial biology. Methods Mol Biol **881:**375–408. http://dx.doi.org/10.1007/978-1-61779-827-6_13.
49. **Mayali X, Weber PK, Brodie EL, Mabery S, Hoeprich PD, Pett-Ridge J.** 2012. High-throughput isotopic analysis of RNA microarrays to quantify microbial resource use. ISME J **6:**1210–1221. http://dx.doi.org/10.1038/ismej.2011.175.
50. **Orphan VJ, House CH, Hinrichs KU, McKeegan KD, DeLong EF.** 2001. Methane-consuming archaea revealed by directly coupled isotopic and phylogenetic analysis. Science **293:**484–487. http://dx.doi.org/10.1126/science.1061338.
51. **Behrens S, Losekann T, Pett-Ridge J, Weber PK, Ng WO, Stevenson BS, Hutcheon ID, Relman DA, Spormann AM.** 2008. Linking microbial phylogeny to metabolic activity at the single-cell level by using enhanced element labeling-catalyzed reporter deposition fluorescence in situ hy-

bridization (EL-FISH) and NanoSIMS. Appl Environ Microbiol **74:**3143–3150. http://dx.doi.org/10.1128/AEM.00191-08.

52. **Urbach E, Vergin KL, Giovannoni SJ.** 1999. Immunochemical detection and isolation of DNA from metabolically active bacteria. Appl Environ Microbiol **65:**1207–1213.
53. **Goldfarb KC, Karaoz U, Hanson CA, Santee CA, Bradford MA, Treseder KK, Wallenstein MD, Brodie EL.** 2011. Differential growth responses of soil bacterial taxa to carbon substrates of varying chemical recalcitrance. Front Microbiol **2:**94. http://dx.doi.org/10.3389/fmicb.2011.00094.
54. **Hellman M, Berg J, Brandt KK, Hallin S.** 2011. Survey of bromodeoxyuridine uptake among environmental bacteria and variation in uptake rates in a taxonomically diverse set of bacterial isolates. J Microbiol Methods **86:**376–378. http://dx.doi.org/10.1016/j.mimet.2011.05.020.
55. **Nannipieri P, Ascher J, Ceccherini MT, Landi L, Pietramellara G, Renella G.** 2003. Microbial diversity and soil functions. Eur J Soil Sci **54:**655–670. http://dx.doi.org/10.1046/j.1351-0754.2003.0556.x.
56. **Stotzky G, Norman AG.** 1961. Factors limiting microbial activities in soil. I. The level of substrate, nitrogen, and phosphorus. Arch Mikrobiol **40:**341–369.
57. **Manefield M, Griffiths RI, Bailey MJ, Whiteley AS.** 2006. Stable isotope probing: a critique of its use in linking phylogeny and function. Nucleic Acids Prot Soil **8:**205–216. http://dx.doi.org/10.1007/3-540-29449-X_10.
58. **Blazewicz SJ, Schwartz E.** 2011. Dynamics of ^{18}O incorporation from $H_2{}^{18}O$ into soil microbial DNA. Microb Ecol **61:**911–916. http://dx.doi.org/10.1007/s00248-011-9826-7.
59. **Schwartz E.** 2007. Characterization of growing microorganisms in soil by stable isotope probing with $H_2{}^{18}O$. Appl Environ Microbiol **73:**2541–2546. http://dx.doi.org/10.1128/AEM.02021-06.
60. **Nannipieri P, Johnson RL, Paul EA.** 1978. Criteria for measurement of microbial-growth and activity in soil. Soil Biol Biochem **10:**223–229. http://dx.doi.org/10.1016/0038-0717(78)90100-1.
61. **McMahon SK, Wallenstein MD, Schimel JP.** 2009. Microbial growth in Arctic tundra soil at −2 degrees C. Environ Microbiol Rep **1:**162–166. http://dx.doi.org/10.1111/j.1758-2229.2009.00025.x.
62. **Bernard L, Mougel C, Maron PA, Nowak V, Leveque J, Henault C, Haichar FZ, Berge O, Marol C, Balesdent J, Gibiat F, Lemanceau P, Ranjard L.** 2007. Dynamics and identification of soil microbial populations actively assimilating carbon from ^{13}C-labelled wheat residue as estimated by DNA- and RNA-SIP techniques. Environ Microbiol **9:**752–764. http://dx.doi.org/10.1111/j.1462-2920.2006.01197.x.
63. **Haichar FZ, Achouak W, Christen R, Heulin T, Marol C, Marais MF, Mougel C, Ranjard L, Balesdent J, Berge O.** 2007. Identification of cellulolytic bacteria in soil by stable isotope probing. Environ Microbiol **9:**625–634. http://dx.doi.org/10.1111/j.1462-2920.2006.01182.x.
64. **Nottingham AT, Griffiths H, Chamberlain PM, Stott AW, Tanner EVJ.** 2009. Soil priming by sugar and leaf-litter substrates: a link to microbial groups. Appl Soil Ecol **42:**183–190. http://dx.doi.org/10.1016/j.apsoil.2009.03.003.
65. **Peterson BJ, Fry B.** 1987. Stable isotopes in ecosystem studies. Annu Rev Ecol Syst **18:**293–320. http://dx.doi.org/10.1146/annurev.es.18.110187.001453.
66. **Schimel DS.** 1993. Isotopic techniques in plant, soil and aquatic biology, vol 3. Theory and application of tracers. Academic Press, San Diego, CA.
67. **Mayali X, Weber PK, Pett-Ridge J.** 2013. Taxon-specific C/N relative use efficiency for amino acids in an estuarine community. FEMS Microbiol Ecol **83:**402–412. http://dx.doi.org/10.1111/j.1574-6941.12000.x.